Hypertension Research (2019) 42:1485–1494
https://doi.org/10.1038/s41440-019-0257-z

ARTICLE

Dronedarone induces regression of coronary artery remodeling related to better global antioxidant status

Begoña Quintana-Villamandos[1,2] · Laia Pazó-Sayós[1] · Silvia Magdalena Arribas[3] · Pilar Rodríguez-Rodríguez[3] · Rainer H. Böger[4] · Nicole Lüneburg[4] · Emilio Delgado-Baeza[5] · Maria Carmen González[3]

Received: 30 September 2018 / Revised: 5 February 2019 / Accepted: 12 March 2019 / Published online: 16 April 2019

Abstract

Our group previously demonstrated that dronedarone induces regression of left ventricular hypertrophy in spontaneously hypertensive rats (SHRs). We assessed changes in vascular remodeling and oxidative stress following short-term use of this agent. The coronary artery was isolated from 10-month-old male SHRs treated with 100 mg kg^{-1} dronedarone once daily for 14 days (SHR-D group), and age-matched untreated SHRs were used as hypertensive controls. We analyzed the geometry and composition of the artery and constructed dose–response curves for acetylcholine and serotonin (5-HT). We calculated a global score (OXY-SCORE) from plasma biomarkers of oxidative status: carbonyl levels, thiol levels, reduced glutathione levels, total antioxidant capacity, and superoxide anion scavenging activity. Finally, we analyzed asymmetric dimethylarginine (ADMA) concentrations in plasma. Dronedarone significantly decreased wall thickness (medial and adventitial layer thickness and cell count) and the cross-sectional area of the artery. Dronedarone significantly improved endothelium-dependent relaxation and reduced the contraction induced by 5-HT. The OXY-SCORE was negative in the SHR model group (suggesting an enhanced oxidative status) and was positive in the SHR-D group (suggesting enhanced antioxidant defense). Dronedarone significantly decreased the concentrations of ADMA. We conclude that dronedarone improves coronary artery remodeling in SHRs. The better global antioxidant status after treatment with dronedarone and decreased plasma ADMA levels could contribute to the cardiovascular protective effect of dronedarone.

Keywords Asymmetric dimethylarginine · Coronary artery remodeling · Dronedarone · OXY-SCORE · Spontaneously hypertensive rat

Introduction

Dronedarone is the newest antiarrhythmic drug recommended for the treatment of atrial fibrillation [1]. Its cardioprotective effect has been associated with reduced mortality in patients with atrial fibrillation [2]. Our group previously demonstrated that 2 weeks of treatment with dronedarone decreases arterial blood pressure and produces regression of left ventricular hypertrophy in spontaneously hypertensive rats (SHRs) [3]. However, changes in vascular remodeling and oxidative stress following short-term use of this agent have not been analyzed to date.

Hypertension leads to adverse remodeling in the coronary artery and therefore increases the incidence of cardiovascular events [4, 5]. Antiarrhythmic therapy and antihypertensive therapy (with β-adrenergic blockers, angiotensin-converting enzyme [ACE] inhibitors, angiotensin receptor antagonists, and calcium channel blockers) reverse vascular remodeling, thus reducing cardiovascular

✉ Begoña Quintana-Villamandos
begoquinti@gmail.com

1 Department of Anesthesiology, Hospital General Universitario Gregorio Marañón, Madrid, Spain

2 Department of Pharmacology and Toxicology, Faculty of Medicine, Universidad Complutense, Madrid, Spain

3 Department of Physiology, Faculty of Medicine, Universidad Autónoma de Madrid, Madrid, Spain

4 Department of Clinical Pharmacology and Toxicology, University Medical Center Hamburg-Eppendorf, Hamburg, Germany

5 Molecular Biology Laboratory, Department of Experimental Medicine and Surgery, Hospital General Universitario Gregorio Marañón, Madrid, Spain

morbidity [6, 7]. This effect may be mediated, in part, by decreases in vascular oxidative stress [8–10]. In fact, antioxidant therapy seems to be a useful strategy for restoring the impaired balance between oxidants and antioxidants in hypertensive conditions. Propranolol inhibits oxidative stress and reduces lipid peroxidation in tissue, carvedilol reduces lipid peroxidation by acting as a free radical scavenger, celiprolol reduces generation of superoxide anions, nebivolol increases nitric oxide (NO) levels and expression of endothelial NO synthase, amlodipine decreases oxidative stress by decreasing malondialdehyde and increasing Na+ K+ ATPase and superoxide dismutase (SOD) levels, and captopril exerts a protective effect owing to the free radical scavenging properties of the thiol residues contained in the drug structure [11]. In addition, asymmetric dimethylarginine (ADMA), a biomarker of vascular disease [12], is elevated in patients with hypertension and coronary artery disease [13–16]. Several studies have shown changes in vascular remodeling and decreased ADMA levels after antihypertensive and antiarrhythmic therapy [17–20].

This study was designed to evaluate the efficacy of dronedarone in attenuating coronary artery remodeling (with regards to structure and function) in SHRs, the most widely used animals for assessment of human essential hypertension. We also explored whether the protective effect of dronedarone could be related to decreases in ADMA levels and oxidative stress. We assessed plasma biomarkers of oxidative damage (OXY) and antioxidant capacity and used them to calculate a global score (OXY-SCORE).

Methods

Design of experiments

The study was performed in accordance with European Union Guidelines for the Care and Use of Laboratory Animals (Directive 2010/63/EU and Spanish RD 53/2013) and was approved by the Ethics Review Board of Hospital General Universitario Gregorio Marañon and by the local government (Comunidad Autónoma de Madrid).

The experiments were performed on 10-month-old male SHRs ($n = 45$) and age-matched normotensive control Wistar-Kyoto rats (WKY rats, $n = 18$) from the colony maintained at the Animal House Facility of the Universidad Autónoma de Madrid (EX/021-U). The four experimental groups used included an untreated WKY group ($n = 18$), an untreated SHR group ($n = 18$), a group of SHRs treated with hydralazine (SHR-H group, $n = 9$), and a group of SHRs treated with dronedarone (SHR-D group, $n = 18$). Dronedarone (100 mg kg^{-1}), hydralazine (14 mg kg^{-1}), or saline solution (control) was administered once daily for 14 days. When treatment was complete, blood samples were taken to study oxidative stress. The rats were sedated with an intraperitoneal injection of diazepam (4 mg kg^{-1}) and ketamine (10 mg kg^{-1}), and sacrificed by decapitation. The coronary arteries were dissected to perform vascular reactivity experiments and to study vascular structure.

Blood pressure and heart rate (HR) measurements

Systolic arterial pressure (SAP) and HR were measured in conscious WKY, SHR, and SHR-D group rats before and after treatment using the tail-cuff method with a photoelectric sensor (Niprem 546, Cibertec, Madrid, Spain).

Confocal microscopy for the study of coronary artery structure

To study the geometry and composition of the coronary artery, we used 9 animals from each group. Briefly, segments of the left anterior descending artery (1 mm in length) were fixed in 4% paraformaldehyde before being washed in 9% saline solution and stained with the nuclear dye DAPI (1:500 of a 5 mg mL^{-1} stock solution). The segments were studied as described elsewhere [19]. A ring and two longitudinal sections were cut from each segment and mounted on a slide in a small well made of spacers to avoid vessel compression. The well was filled with mounting medium (Citifluor, Aname, Spain). One longitudinal section was mounted with the endothelial side up, and the other was mounted with the adventitial side up. Both sections were studied with a Leica TCS SP2 confocal system (Leica Microsystems, Wetzlar, Germany) at an excitation wavelength of 405 nm and an emission wavelength of 410–475 nm to visualize the cell nuclei. In each artery, three randomly selected regions were visualized with a ×20 objective at zoom 8. In each of these regions, stacks of serial 1-μm optical sections were captured from the adventitial and medial layers. The rings were visualized with a ×20 objective at the 488/515 nm line, and an image was captured to quantify the internal diameter (calculated from the internal perimeter).

Quantitative analysis was performed using MetaMorph Image Analysis Software (Universal Imaging, Wokingham, UK) as previously described [21]. The thickness of each layer in micrometer was determined by the number of planes between the first image showing an adventitial cell and the last image showing a smooth muscle cell (SMC) at the maximum intensity, and by the number of planes between the first image showing the first SMC and the last image showing the first endothelial cell. Adventitial cells and SMCs were counted in a specific volume defined by the image area (8731.03 μm^2 for a ×20 objective at zoom 8) and the layer thickness of each particular vessel. The data

obtained included the adventitial and medial thickness, cell count, cellular density, external diameter (internal diameter + adventitial layer + medial layer), and cross-sectional area (CSA, adventitial layer + medial layer).

Wire myography for the study of coronary artery function

We studied the reactivity of the coronary artery using 9 animals from each group. The heart was removed and maintained in cold (4 °C), oxygenated Krebs–Henseleit solution (KHS, in mmol L^{-1}: 115 NaCl, 25 $NaHCO_3$, 4.7 KCl, 1.2 $MgSO_4 \cdot 7H_2O$, 2.5 $CaCl_2$, 1.2 KH_2PO_4, 11.1 glucose, and 0.01 Na_2EDTA). Segments of the left anterior descending artery (2 mm in length) were isolated, mounted on a wire myograph (Multi Myograph System, model 610M; Danish Myo-Technology) coupled to a PowerLab data acquisition system (ADInstruments, Castle Hill, Australia), and studied as previously described [8, 19]. Responses to acetylcholine (ACh, to assess endothelium-dependent relaxation; 10^{-9}–10^{-4} mol L^{-1}) were studied in segments precontracted with 5-hydroxytryptamine (5-HT, 3×10^{-7} mol L^{-1}). Relaxation responses are expressed as the percent reduction from the 5-HT precontracted state. After a washout period of 60 min, concentration–response curves after application of 5-HT (10^{-9}–3×10^{-5} mol L^{-1}) were plotted for the same arteries. Contraction with 5-HT is expressed as a percentage of the maximum response of the arteries to K^+-KHS. Dose–response curves were then constructed for sodium nitroprusside (SNP, 10^{-9}–10^{-4} mol L^{-1}) to study endothelium-independent relaxation in segments precontracted with 5-HT (3×10^{-7} mol L^{-1}).

Biomarkers of oxidative status in plasma

Blood samples (9 animals from each group) were centrifuged at $900 \times g$ for 10 min at 4 °C to obtain plasma.

Total thiols

Plasma thiols were assessed using a 5,5′-dithiobis (2-nitrobenzoic acid) assay [22] adapted for nanovolumes. Absorbance was measured at 412 nm in a NanoDrop 2000 spectrophotometer (Thermo Scientific, MA, USA).

Total antioxidant capacity (TAC)

TAC was assessed using a CUPRAC-BCS assay [23] adapted to nanovolumes. Absorbance at 490 nm was read in a NanoDrop 2000 spectrophotometer (Thermo Scientific, MA, USA). TAC values were obtained from the standard curve of the antioxidant Trolox (0–2 mol L^{-1})

Quantification of superoxide anion scavenging activity (SOSA)

SOSA was determined using a luminescence assay with coelenterazine as the detection probe [24] adapted to a microplate reader. SOSA values were quantified by comparing the inhibition of luminescence for each sample with that observed from the SOD activity standard curve (0–4 U mL^{-1})

Reduced glutathione (GSH) content

Plasma GSH was assessed using a fluorometric micromethod based on a reaction with *o*-phthalaldehyde [25, 26]. Fluorescence was measured in a Synergy HT Multi-Mode Microplate Reader (Biotek) at an excitation wavelength of 360 ± 40 nm and an emission wavelength of 460 ± 40 nm.

Total protein carbonyls

Total protein carbonyls were quantified using a simplified 2,4-dinitrophenylhydrazine (DNPH) spectrophotometric assay [27], which was adapted for nanovolumes. Absorbance at 450 nm was read in a NanoDrop 2000 spectrophotometer (Thermo Fisher Scientific, MA, USA). Protein carbonyl levels were calculated using the extinction coefficient of DNPH at 450 nm ($\varepsilon = 22{,}308\ M^{-1}\ cm^{-1}$) and an optical path length of 1 mm and are expressed as nanomoles of carbonyls per milligram protein. The amount of total protein in the samples was assessed using Bradford reagent according to the manufacturer's recommendations (Bio-Rad, USA).

Protein content

Protein content was assessed using a Coomassie blue-based microtiter plate assay according to the manufacturer's recommendations (Bio-Rad, Madrid, Spain). Absorbance was measured at 595 nm in a Synergy HT Multi-Mode Microplate Reader (Bio-Tek), and bovine serum albumin was used as the standard.

Calculation of the OXY-SCORE

Biomarkers related to antioxidant defense systems (ANTIOX) and OXY were used to calculate the OXY-SCORE associated with the administration of dronedarone. First, we analyzed the normality of the chosen oxidative stress biomarkers using the Kolmogorov–Smirnov test (the parameters that did not show a normal distribution were normalized through a logarithmic transformation). We then standardized the parameters and calculated the partial indexes for OXY and ANTIOX, as well as the OXY-SCORE according to a previously described methodology

[28]. Based on this calculation, a positive OXY-SCORE indicates a predominance of antioxidant capacity, and a negative OXY-SCORE indicates a predominance of OXY.

Measurement of ADMA concentrations in plasma

We analyzed five animals from each group. Mass spectrometry of ADMA was performed as previously described using a fully validated high-throughput liquid chromatography/tandem mass spectrometry assay [29, 30].

Statistical analysis

The results are expressed as the mean ± SEM. The parameters were compared using repeated-measures analysis of variance (for concentration–response curve parameters) and single-factor (rat) analysis of variance (for physiological, structural, and biochemical parameters). With regards to the responses to ACh, 5-HT, and SNP in coronary segments, some results are expressed as differences in the areas under the concentration–response curves (AUCs) among the experimental groups. P-values < 0.05 were considered to indicate statistical significance. Statistical analysis was performed using IBM SPSS Statistics for Windows, version 20.0 (IBM Corp., Armonk, NY, USA) and GraphPad Prism 6.0 (GraphPad Software, CA, USA).

Results

Treatment with dronedarone for 2 weeks decreases arterial pressure and HR

The weight of WKY rats was significantly greater than that of SHR group rats (431.40 ± 3.21 versus 381.63 ± 7.21 g, $P < 0.01$), SHR-H group rats (431.40 ± 3.21 versus 375.13 ± 5.11 g, $P < 0.01$), and SHR-D group rats (431.40 ± 3.21 versus 360.16 ± 3.41 g, $P < 0.001$). No statistically significant differences in rat weight were observed among the SHR, SHR-H, and SHR-D groups. SAP was significantly higher in the SHR group than in the WKY group (179 ± 21 versus 128 ± 12 mmHg, $P < 0.01$). Dronedarone significantly reduced SAP in the SHR-D group compared with the SHR group (140 ± 11 versus 179 ± 21 mmHg, $P < 0.01$) to values similar to those in the WKY group. The SHR-H group showed the same reduction in SAP as the SHR-D group (146 ± 8 versus 140 ± 11 mmHg). HR was not significantly different among the WKY, SHR, and SHR-H groups. Dronedarone significantly reduced HR in the SHR-D group compared with the control (WKY), SHR, and SHR-H groups (271 ± 31 versus 374 ± 10 bpm, $P < 0.001$; 271 ± 31 versus 397 ± 26 bpm, $P < 0.001$; 271 ± 31 versus 383 ± 21 bpm, $P < 0.001$).

Treatment with dronedarone for 2 weeks improves anterior descending artery structure

The effects of dronedarone on coronary artery geometry are shown in Fig. 1. The SHR group presented hypertrophic outward remodeling associated with a significant increase in CSA (Fig. 1a) and LD (Fig. 1b) in the anterior descending coronary artery when compared with the WKY group. After 2 weeks of treatment with dronedarone, CSA and WW (Fig. 1c) were significantly lower in the SHR-D group than in the SHR group, but no differences were observed with respect to the WKY group. LD in the SHR group-D did not differ from that in the SHR group. ED (Fig. 1d) was significantly higher in the SHR group than in the WKY group; however, administration of dronedarone significantly decreased this parameter in the SHR-D group compared with the SHR group. There were no significant differences in LD, CSA, WW, and ED between the SHR and SHR-H groups.

The effects of dronedarone on coronary artery composition (medial and adventitial layer) are shown in Figs. 2 and 3. The medial layer thickness (Fig. 2a, c) and SMC count (Fig. 2b) were significantly higher in the SHR group than in the WKY group, although dronedarone significantly lowered both parameters in the SHR-D group compared to the SHR group. There were no significant differences in the medial layer (in wall thickness, SMC count, or cell density) between the SHR-D and WKY groups (Fig. 2c). There were no significant differences in the medial layer (in wall thickness or SMC count) between the SHR and SHR-H groups. There were no significant differences in medial cell density among the four experimental groups. The adventitia contained significantly more cells in the SHR group than in the WKY group. However, 2 weeks of treatment with dronedarone induced a significant reduction in wall thickness and cell count in the SHR-D group compared with the SHR group (Fig. 3a, b). Consequently, cell density was significantly higher in the SHR-D group than in control group (Fig. 3b). There were no significant differences in the adventitial layer (in wall thickness, SMC count, or adventitial cell density) between the SHR and SHR-H groups.

Treatment with dronedarone for 2 weeks improves anterior descending artery vascular reactivity

Vasodilator function

KCl-induced contraction was not significantly different among the four experimental groups (WKY: 1.54 ± 0.24 mN mm^{-1}, SHR: 1.24 ± 0.31 mN mm^{-1}, SHR-H: 1.20 ± 0.11 mN mm^{-1}, and SHR-D: 1.17 ± 0.25 mN mm^{-1}). No differences in the concentration–response curves for the endothelium-independent vasodilator SNP (10^{-9}–10^{-4} mol L^{-1}) were observed among the four experimental groups.

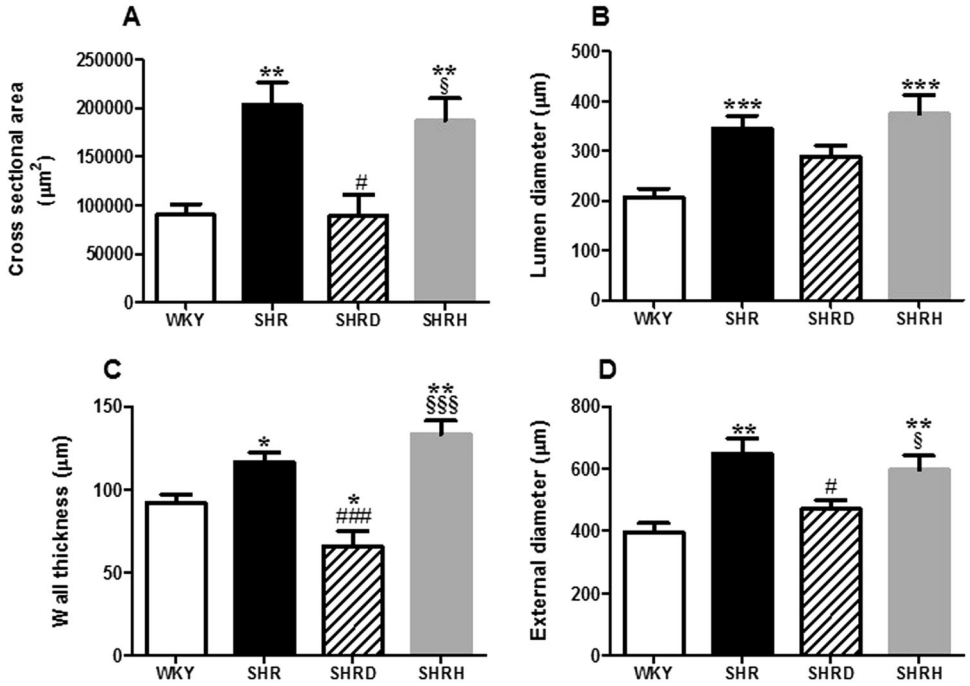

Fig. 1 Structural parameters (medial + adventitial layers). Shown are the cross-sectional area (**a**), lumen diameter (**b**), wall thickness (**c**), and external diameter (**d**) of the coronary artery from Wistar Kyoto rats (WKY group), spontaneously hypertensive rats (SHRs; SHR group), SHRs treated with dronedarone (SHR-D group), and SHRs treated with hydralazine (SHR-H group). $N = 9$ rats for each experimental group. The data are expressed as the mean ± SEM. Statistically significant differences among the WKY, SHR, SHR-D, and SHR-H groups are shown ($^{*}P < 0.05$ versus WKY; $^{**}P < 0.01$ versus WKY; $^{***}P < 0.001$ versus WKY; $^{\#}P < 0.05$ versus SHR; $^{\#\#\#}P < 0.001$ versus SHR; $^{\S}P < 0.05$ versus SHR-D; $^{\S\S\S}P < 0.001$ versus SHR-D)

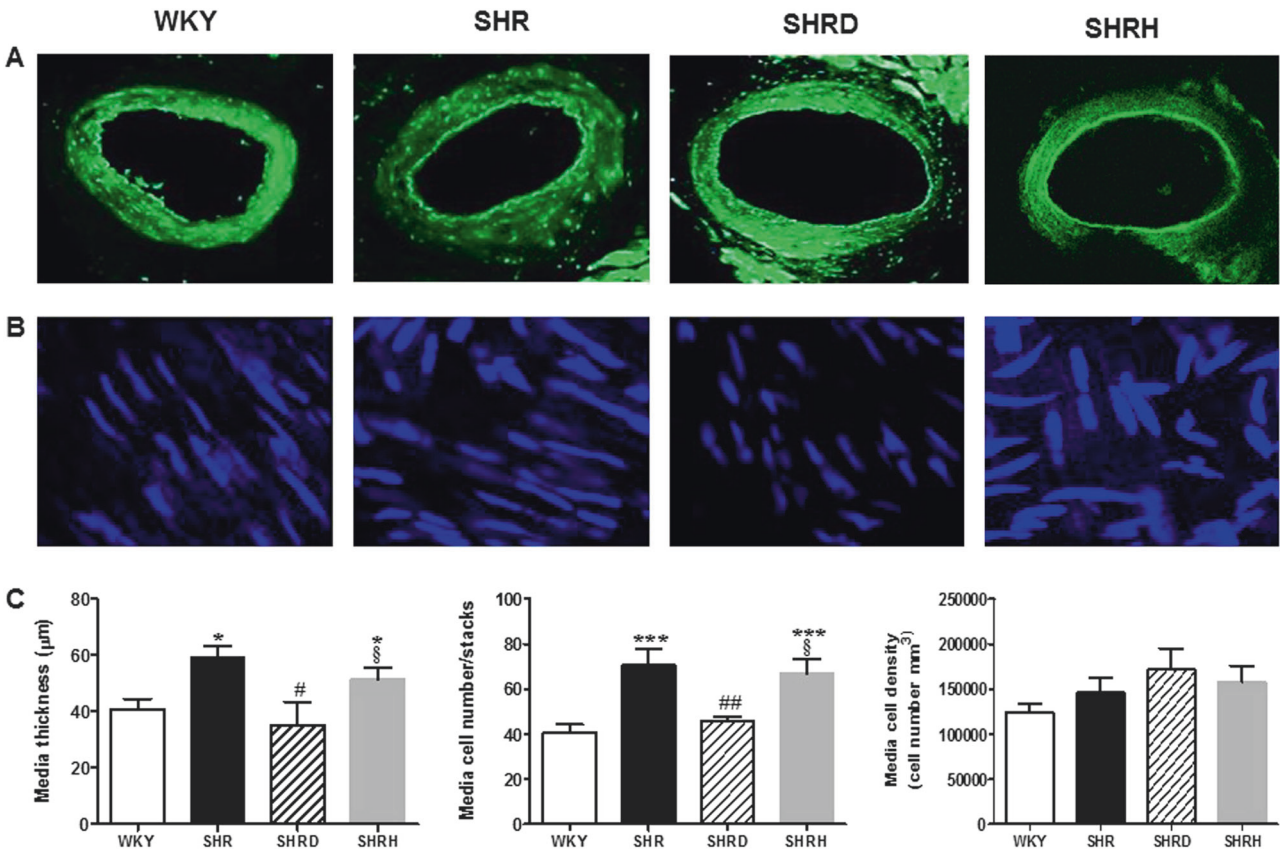

Fig. 2 Medial layer of the coronary artery. Shown are rings (examples of projections obtained from confocal microscopy images, ×20, zoom 2) (**a**), cell nuclei (examples of projections obtained from confocal microscopy images, ×20, zoom 8) (**b**), and the composition of the medial layer (medial thickness, medial cell number, and medial cell density) (**c**) of the coronary artery from Wistar Kyoto rats (WKY group), spontaneously hypertensive rats (SHRs; SHR group), SHRs treated with dronedarone (SHR-D group), and SHRs treated with hydralazine (SHR-H group). $N = 9$ rats for each experimental group. The data are expressed as the mean ± SEM. Statistically significant differences among the WKY, SHR, SHR-D, and SHR-H groups are shown ($^{*}P < 0.05$ versus WKY; $^{***}P < 0.001$ versus WKY; $^{\#}P < 0.05$ versus SHR; $^{\#\#}P < 0.01$ versus SHR; $^{\S}P < 0.05$ versus SHR-D)

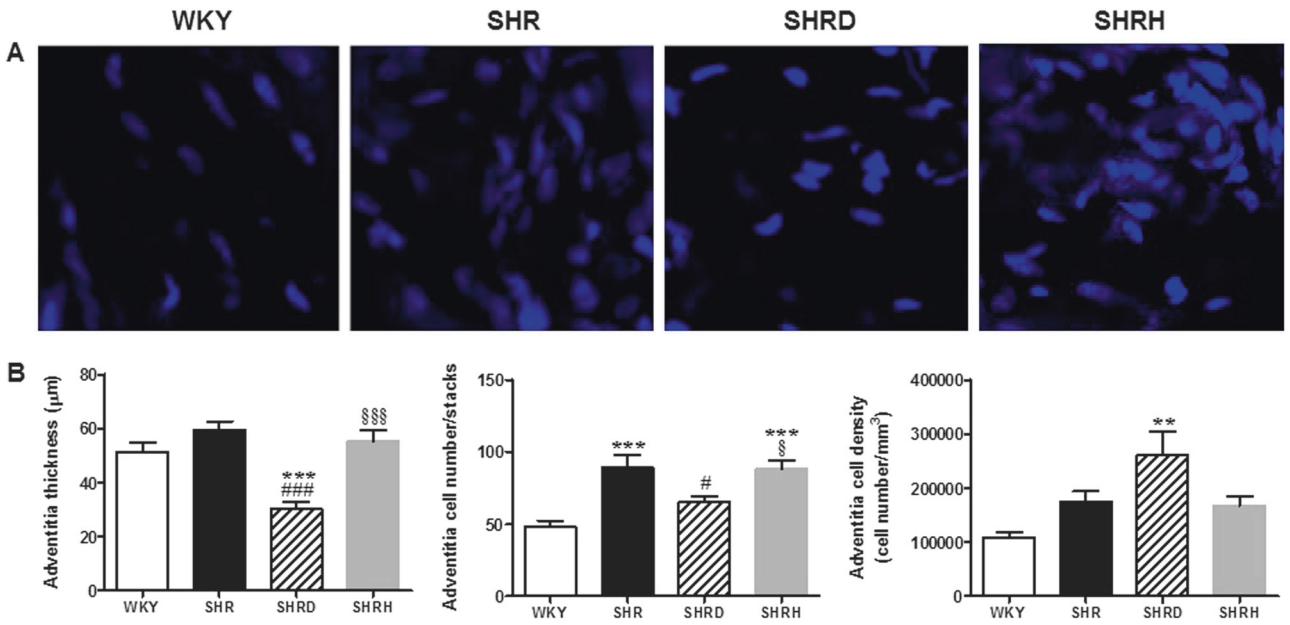

Fig. 3 Adventitial layer of the coronary artery. Shown are cell nuclei (examples of projections obtained from confocal microscopy images, ×20, zoom 8) (**a**) and the composition of the adventitial layer (adventitial thickness, adventitial cell count, and adventitial cell density) (**b**) of the coronary artery from Wistar Kyoto rats (WKY group), spontaneously hypertensive rats (SHRs; SHR group), SHRs treated with dronedarone (SHR-D group), and SHRs treated with hydralazine (SHR-H group). $N = 9$ rats for each experimental group. The data are expressed as the mean ± SEM. Statistically significant differences among the WKY, SHR, SHR-D, and SHR-H groups are shown ($^{**}P < 0.01$ versus WKY; $^{***}P < 0.001$ versus WKY; $^{\#}P < 0.05$ versus SHR; $^{\#\#\#}P < 0.001$ versus SHR; $^{\S}P < 0.05$ versus SHR-D; $^{\S\S\S}P < 0.001$ versus SHR-D)

In the WKY group, ACh elicited concentration-dependent relaxation at all concentrations (10^{-9}–10^{-4} mol L^{-1}), whereas in the SHR group, ACh elicited dilatation at low concentrations (10^{-9}–10^{-7} mol L^{-1}) and contractions at higher concentrations (10^{-4} mol L^{-1}). Dronedarone significantly improved the endothelium-dependent relaxation induced by ACh at low concentrations (10^{-9}–10^{-7} mol L^{-1}) in the SHR-D group compared to the SHR group (Fig. 4a). The AUC was significantly greater in the WKY group than in the SHR group. Dronedarone produced a significantly higher AUC in the SHR-D group than in the SHR group. Vasodilator function was normalized by dronedarone. No differences were observed between the SHR and SHR-H groups (Fig. 4a).

Contractile response

The contractile response to 5-HT (3×10^{-8}–3×10^{-5} mol L^{-1}) was significantly higher in the SHR group than in the WKY group. Dronedarone significantly reduced the contraction induced by 5-HT (3×10^{-7}–3×10^{-5} mol L^{-1}) in the SHR-D group compared to the SHR group (Fig. 4b). The AUC was significantly greater in the SHR group than in the WKY group and was significantly lower in the SHR-D group than in the SHR group. No differences were observed between the SHR-D and WKY groups. No differences were observed between the SHR and SHR-H groups (Fig. 4b).

Dronedarone improves plasma redox status

The effects of dronedarone on plasma biomarkers related to ANTIOX (total thiols, GSH, TAC, SOD) and OXY (protein carbonyls) are shown in Fig. 5. These parameters were used to calculate a global index of oxidative stress (OXY-SCORE). The OXY-SCORE was calculated from the normalized and standardized plasma parameters. SOSA and TAC did not exhibit a normal distribution and were therefore normalized by a logarithmic transformation before being standardized. The SHR group had a negative OXY-SCORE value, thus indicating an imbalance between oxidative status and ANTIOX with increased oxidative status. However, in the SHR-D group, the OXY-SCORE value was positive, suggesting enhanced antioxidant defense. The OXY-SCORE was significantly lower in the SHR group than in the SHR-D group ($P < 0.001$) (Fig. 6a).

Dronedarone decreases plasma concentrations of ADMA

Plasma concentrations of ADMA were significantly higher in the SHR group than in the WKY group. Treatment with dronedarone significantly decreased plasma concentrations of ADMA in the SHR-D group compared to the SHR group. No differences were observed when the SHR-D group was compared with the WKY group (Fig. 6b).

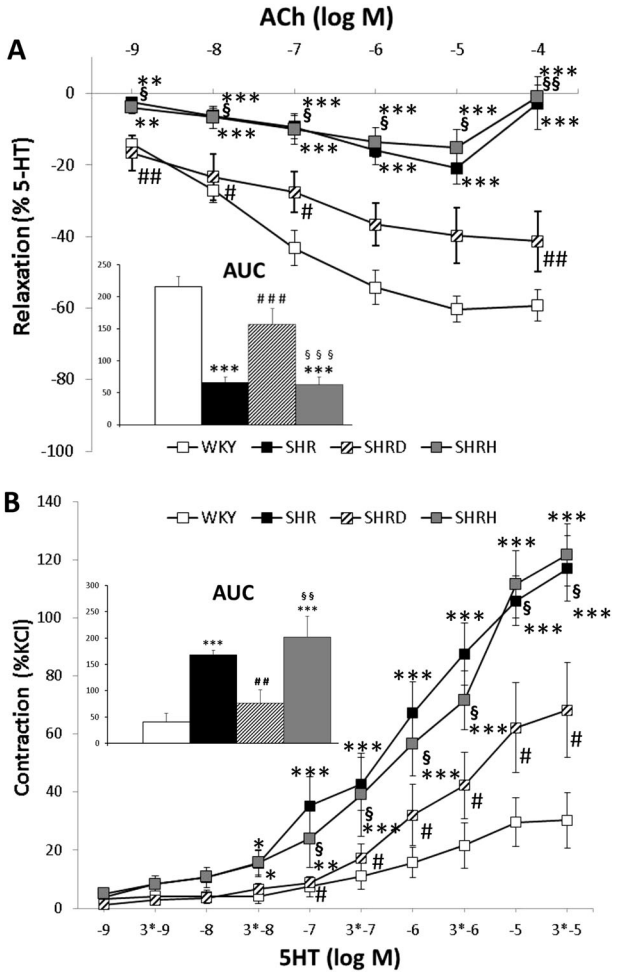

Fig. 4 Vascular reactivity parameters. Shown are acetylcholine (ACh, 10^{-9}–10^{-4} mol L^{-1}) responses in the coronary artery precontracted with 5-hydroxytryptamine (5-HT) and the areas under the concentration–response curves (AUCs) for Ach (**a**) from Wistar Kyoto rats (WKY group), spontaneously hypertensive rats (SHRs; SHR group), SHRs treated with dronedarone (SHR-D group), and SHRs treated with hydralazine (SHR-H group). Relaxation responses are expressed as the percent reductions from the 5-HT–precontracted state. 5-HT (5-HT, 10^{-9}–3×10^{-5} mol L^{-1}) responses in the coronary artery and the areas under the concentration–response curve (AUCs) for 5-HT (**b**) from the WKY, SHR, SHR-D, and SHR-H groups are also shown. Contraction responses with 5-HT are expressed as the percentages of the maximum response of the arteries to K+-KHS. $N = 9$ rats for each experimental group. The data are expressed as the mean ± SEM. Statistically significant differences among the WKY, SHR, SHR-D, and SHR-H groups are shown ($^{*}P < 0.05$ versus WKY; $^{**}P < 0.01$ versus WKY; $^{***}P < 0.001$ versus WKY; $^{\#}P < 0.05$ versus SHR; $^{\#\#}P < 0.01$ versus SHR; $^{\S}P < 0.05$ versus SHR-D; $^{\S\S}P < 0.01$ versus SHR-D)

Discussion

Our results show that 2 weeks of treatment with dronedarone improves coronary artery remodeling in adult SHRs. The improved global antioxidant status after treatment with dronedarone and decreased ADMA levels could contribute to the cardiovascular protective effect of the drug.

Our group previously demonstrated that dronedarone produces regression of left ventricular hypertrophy in SHRs [3]. In fact, functional and structural alterations in coronary circulation have been well documented in left ventricular hypertrophy [4]. Thus, in the present study, we show changes in the structure and function of the anterior descending coronary artery after treatment with dronedarone. This protective effect following regression of coronary artery remodeling has been reported with antihypertensive and antiarrhythmic drugs administered over several months in SHRs (β-adrenergic blockers, ACE inhibitors, angiotensin receptor antagonists, and calcium channel blockers) [17, 31–33]. Dronedarone improved vascular wall structure and morphology and attenuated coronary artery dysfunction after only 2 weeks of treatment [8, 19].

Dronedarone is an interesting antiarrhythmic agent for the treatment of atrial fibrillation [2, 34, 35]. Although its mechanism of action is not completely clear, we do know that the drug reduces the risk of acute coronary syndrome. Three mechanisms contribute to the beneficial effects of dronedarone in acute coronary syndrome [36]. First, dronedarone reduces HR, thus reducing myocardial oxygen consumption. Second, dronedarone decreases vasoconstriction and thus reduces arterial pressure through inhibition of α-adrenoceptors. Third, dronedarone has a direct cardioprotective effect (it reduces infarct size in an animal ischemia/reperfusion model).

Increases in NO have been reported by other investigators, who have demonstrated that dronedarone stimulates the nitric oxide synthase (NOS) pathway [37]. NO inhibits proliferation of SMCs [38] and thus has a protective effect on vascular remodeling (decreasing wall thickness) because SMCs participate in hypertrophy of the arterial wall (the tunica media accounts for ~95% of the arterial wall in SHRs) [17]. Therefore, in the present study, the mechanism underlying the dronedarone-induced protective effects, namely, regression of vascular remodeling in coronary arteries, could be related in part to increases in the bioavailability of NO. This hypothesis could be supported by our finding of a decrease in plasma concentrations of ADMA after treatment with dronedarone. ADMA is a novel marker of the risk of cardiovascular disease [39]. In a preclinical study with SHRs, we elucidated the association between ADMA and cardiovascular remodeling [40]. ADMA reduces the production of NO by inhibiting the activity of NOS and therefore increasing the proliferation of vascular SMCs [12, 39]. Several studies have shown that changes in vascular remodeling lead to decreases in ADMA levels after antihypertensive and antiarrhythmic therapy (with losartan, nebivolol, and esmolol) [17–20, 41]. This finding could explain the regression of coronary artery remodeling by dronedarone. However, the molecular

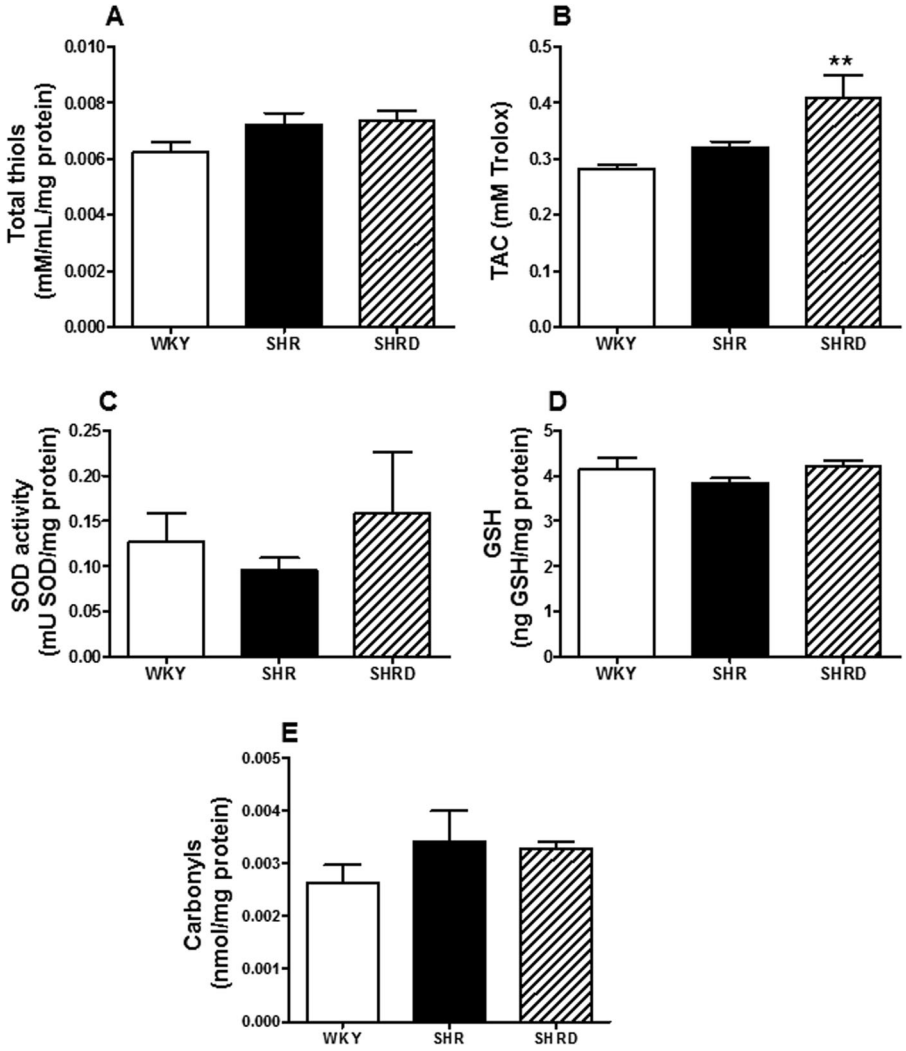

Fig. 5 Oxidative status biomarkers. Total thiols (**a**), total antioxidant capacity (TAC) (**b**), superoxide dismutase (SOD) (**c**), reduced glutathione (GSH) (**d**), and carbonyls (**e**) in plasma from Wistar Kyoto rats (WKY group), spontaneously hypertensive rats (SHRs; SHR group), and SHRs treated with dronedarone (SHR-D group) are shown. $N = 9$ rats for each experimental group. The data are expressed as the mean ± SEM. Statistically significant differences among the WKY, SHR, and SHR-D groups are shown ($^{**}P < 0.01$ versus WKY)

mechanism responsible for the reduction in ADMA levels mediated by dronedarone remains unknown.

Hypertension is associated with cardiovascular remodeling and endothelial dysfunction, alterations in which oxidative stress plays a key role [42–45]. Antihypertensive and antiarrhythmic drugs (such as nifedipine, amlodipine, perindopril, telmisartan, and esmolol) improve vascular structure and function, in part by decreasing vascular oxidative stress and increasing antioxidant capacity [8, 46]. Other pharmacological agents decrease oxidative stress and provide vasoprotection [47]. Dronedarone has been associated with a reduction in oxidative stress-related microvascular abnormalities in a porcine model of rapid atrial pacing; therefore, dronedarone improves ventricular circulation [48]. To investigate the potential of dronedarone for reducing oxidative stress-related coronary artery remodeling in SHRs, we measured plasma TAC and plasma levels of GSH, SOD, and protein carbonyls because a good correlation has been reported between the levels of these biomarkers in plasma and their levels in several tissues, including heart tissue [49]. In fact, oxidative stress has been implicated in hypertension and cardiovascular remodeling [50]; however, a specific biomarker does not provide information on global oxidative status. In the literature, in human and preclinical studies, global scores based on individual plasma biomarkers of antioxidant defense and OXY have been calculated to assess the overall oxidative balance in cardiovascular disease [22, 51, 52]. Our study shows that dronedarone is associated with improved global oxidative status in plasma. This enhanced antioxidant defense could be involved in the causal relationship between dronedarone treatment and decreases in plasma ADMA levels [18, 53, 54]. This finding provides a possible explanation for the improvement in coronary artery remodeling in SHRs treated with dronedarone.

In conclusion, dronedarone improves coronary artery remodeling in SHRs. The improved global antioxidant status after treatment with dronedarone and the decreased ADMA levels could contribute to the cardiovascular protective effect of dronedarone. In the near future, clinical

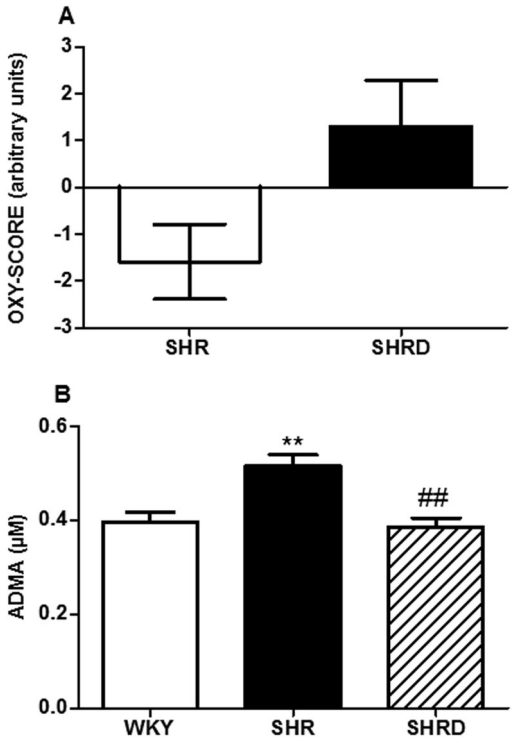

Fig. 6 Global oxidative status score (OXY-SCORE) calculated from the plasma biomarkers of oxidative damage and antioxidant capacity (**a**) from spontaneously hypertensive rats (SHRs; SHR group) and SHRs treated with dronedarone (SHR-D group). $N = 9$ rats for each experimental group. The plasma concentrations of asymmetric dimethylarginine (ADMA) (**b**) from the Wistar Kyoto (WKY) group, the SHR group, and the SHR-D group are also shown. $N = 5$ rats for each experimental group. The data are expressed as the mean ± SEM. Statistically significant differences among the WKY, SHR, and SHR-D groups are shown ($^{**}P < 0.01$ versus WKY; $^{\#\#}P < 0.01$ versus SHR)

trials should be performed to demonstrate these findings in humans.

Acknowledgements This study was supported by the Spanish Health Ministry (Fondo de Investigaciones Sanitarias) under Contracts FIS 13/01261 and FIS 16/02069 and Fondos FEDER.

Compliance with ethical standards

Conflict of interest The authors declare that they have no conflict of interest.

Publisher's note: Springer Nature remains neutral with regard to jurisdictional claims in published maps and institutional affiliations.

References

1. Tadros R, Nattel S, Andrade JG. Dronedarone: basic pharmacology and clinical use. Card Electrophysiol Clin. 2016;8:453–65.
2. Lee EJ, Kim J. Evaluation of dronedarone as a therapeutic option for patients with atrial fibrillation. J Clin Pharm Ther. 2014;39:112–7.
3. Quintana-Villamandos B, Gomez de Diego JJ, Delgado-Martos MJ, Muñoz-Valverde D, Soto-Montenegro ML, Desco M, et al. Dronedarone produces early regression of myocardial remodelling in structural heart disease. PLoS ONE. 2017;12:e0188442.
4. Camici PG, Olivotto I, Rimoldi OE. The coronary circulation and blood flow in left ventricular hypertrophy. J Mol Cell Cardiol. 2012;52:857–64.
5. Intengan HD, Schiffrin EL. Vascular remodeling in hypertension: roles of apoptosis, inflammation, and fibrosis. Hypertension. 2001;38:581–7.
6. Rehman A, Schiffrin EL. Vascular effects of antihypertensive drug therapy. Curr Hypertens Rep. 2010;12:226–32.
7. Schiffrin EL. Vascular remodeling and endothelial function in hypertensive patients: effects of antihypertensive therapy. Scand Cardiovasc J Suppl. 1998;47:15–21.
8. Arnalich-Montiel A, González MC, Delgado-Baeza E, Delgado-Martos MJ, Condezo-Hoyos L, Martos-Rodríguez A, et al. Short-term esmolol improves coronary artery remodeling in spontaneously hypertensive rats through increased nitric oxide bioavailability and superoxide dismutase activity. Biomed Res Int. 2014;2014:531087.
9. Oudot A, Vergely C, Ecarnot-Laubriet A, Rochette L. Angiotensin II activates NADPH oxidase in isolated rat hearts subjected to ischaemia-reperfusion. Eur J Pharmacol. 2003;462:145–54.
10. Ghiadoni L, Magagna A, Versari D, Kardasz I, Huang Y, Taddei S, et al. Different effect of antihypertensive drugs on conduit artery endothelial function. Hypertension. 2003;41:1281–6.
11. Sorriento D, De Luca N, Trimarco B, Iaccarino G. The antioxidant therapy: new insights in the treatment of hypertension. Front Physiol. 2018;9:258.
12. Cooke JP. ADMA: its role in vascular disease. Vasc Med. 2005;10(Suppl. 1):S11–S17.
13. Surdacki A, Nowicki M, Sandmann J, Tsikas D, Kruszelnicka-Kwiatkowska O, Kokot F, et al. Reduced urinary excretion of nitric oxide metabolites and increased plasma levels of asymmetric dimethylarginine in men with essential hypertension. J Cardiovasc Pharmacol. 1999;33:652–8.
14. Perticone F, Sciacqua A, Maio R, Perticone M, Maas R, Boger RH, et al. Asymmetric dimethylarginine, L-arginine, and endothelial dysfunction in essential hypertension. J Am Coll Cardiol. 2005;46:518–23.
15. Valkonen VP, Päivä H, Salonen JT, Lakka TA, Lehtimäki T, Laakso J, et al. Risk of acute coronary events and serum concentration of asymmetrical dimethylarginine. Lancet. 2001;358:2127–8.
16. Lu TM, Ding YA, Charng MJ, Lin SJ. Asymmetrical dimethylarginine: a novel risk factor for coronary artery disease. Clin Cardiol. 2003;26:458–64.
17. Koprdova R, Cebova M, Kristek F. Long-term effect of losartan administration on blood pressure, heart and structure of coronary artery of young spontaneously hypertensive rats. Physiol Res. 2009;58:327–35.
18. Li D, Xia K, Li NS, Luo D, Wang S, Jiang DJ, et al. Reduction of asymmetric dimethylarginine involved in the cardioprotective effect of losartan in spontaneously hypertensive rats. Can J Physiol Pharmacol. 2007;85:783–9.
19. Quintana-Villamandos B, Arnalich-Montiel A, Arribas S, Lüneburg N, Böger RH, Delgado-Martos MJ, et al. Esmolol produces regression of coronary artery remodeling in hypertensive rats: role of ADMA. Hypertens Res. 2016;39:692–700.
20. Wang Y, Zhang M, Liu Y, Liu Y, Chen M. The effect of nebivolol on asymmetric dimethylarginine system in spontaneously hypertension rats. Vasc Pharmacol. 2011;54:36–43.
21. Conde MV, Gonzalez MC, Quintana-Villamandos B, Abderrahim F, Briones AM, Condezo-Hoyos L, et al. Liver growth factor treatment restores cell-extracellular matrix balance in resistance

arteries and improves left ventricular hypertrophy in SHR. Am J Physiol Heart Circ Physiol. 2011;301:H1153–H1165.
22. Condezo-Hoyos L, Rubio M, Arribas SM, España-Caparrós G, Rodríguez-Rodríguez P, Mujica-Pacheco E, et al. A plasma oxidative stress global index in early stages of chronic venous insufficiency. J Vasc Surg. 2013;57:205–13.
23. Campos C, Guzman R, Lopez-Fernandez E, Casado A. Evaluation of the copper (II) reduction assay using bathocuproinedisulfonic acid disodium salt for the total antioxidant capacity assessment: the CUPRAC-BCS assay. Anal Biochem. 2009;392:37–44.
24. Saleh L, Plieth C. A coelenterazine-based luminescence assay to quantify high-molecular-weight superoxide anion scavenger activities. Nat Protoc. 2010;5:1635–41.
25. Hissin PJ, Hilf R. A fluorometric method for determination of oxidized and reduced glutathione in tissues. Anal Biochem. 1976;74:214–26.
26. Jia Z, Saha S, Zhu H, Li Y, Misra HP. Spectrofluorometric measurement of reduced glutathione levels in human neuronal cells. In: Dap DK, (Ed.). Methods redox signal. New York, USA: Mary Ann Liebert Inc; 2010. p. 235–7.
27. Mesquita CS, Oliveira R, Bento F, Geraldo D, Rodrigues JV, Marcos JC. Simplified 2,4-dinitrophenylhydrazine spectrophotometric assay for quantification of carbonyls in oxidized proteins. Anal Biochem. 2014;458:69–71.
28. Veglia F, Cavalca V, Tremoli E. OXY-SCORE: a global index to improve evaluation of oxidative stress by combining pro- and antioxidant markers. Methods Mol Biol. 2010;594:197–213.
29. Schwedhelm E, Tan-Andresen J, Maas R, Riederer U, Schulze F, Böger RH. Liquid chromatography-tandem mass spectrometry method for the analysis of asymmetric dimethylarginine in human plasma. Clin Chem. 2005;51:1268–71.
30. Schwedhelm E, Maas R, Tan-Andresen J, Schulze F, Riederer U, Böger RH. High-throughput liquid chromatographic-tandem mass spectrometric determination of arginine and dimethylated arginine derivatives in human and mouse plasma. J Chromatogr B. 2007;851:211–9.
31. Sharifi AM, Li JS, Endemann D, Schiffrin EL. Effects of enalapril and amlodipine on small-artery structure and composition, and on endothelial dysfunction in spontaneously hypertensive rats. J Hypertens. 1998;16:457–66.
32. Neglia D, Fommei E, Varela-Carver A, Mancini M, Ghione S, Lombardi M, et al. Perindopril and indapamide reverse coronary microvascular remodelling and improve flow in arterial hypertension. J Hypertens. 2011;29:364–72.
33. Brilla CG, Janicki JS, Weber KT. Impaired diastolic function and coronary reserve in genetic hypertension: Role of interstitial fibrosis and medial thickening of intramyocardial coronary arteries. Circ Res. 1991;69:107–15.
34. Oyetayo OO, Rogers CE, Hofmann PO. Dronedarone: a new antiarrhythmic agent. Pharmacotherapy. 2010;30:904–15.
35. Baroletti S, Catella J, Ehle M, Cheng JWM. Dronedarone: a review of characteristics and clinical data. Crit Pathw Cardiol. 2010;9:94–101.
36. Heijman J, Heusch G, Dobrev D. Pleiotropic effects of antiarrhythmic agents: dronedarone in the treatment of atrial fibrillation. Clin Med Insights Cardiol. 2013;7:127–40.
37. Guiraudou P, Pucheu SC, Gayraud R, Gautier P, Roccon A, Herbert JM, et al. Involvement of nitric oxide in amiodarone- and dronedarone-induced coronary vasodilation in guinea pig heart. Eur J Pharmacol. 2004;496:119–27.
38. Böger RH. Asymmetric dimethylarginine (ADMA) modulates endothelial function-therapeutic implications. Vasc Med. 2003;8:149–51.
39. Sibal L, Agarwal SC, Home PD, Boger RH. The role of asymmetric dimethylarginine (ADMA) in endothelial dysfunction and cardiovascular disease. Curr Cardiol Rev. 2010;6:82–90.
40. Quintana-Villamandos B, Delgado-Baeza E. Does the ADMA/DDAH/NO pathway modulate early regression of left ventricular hypertrophy with esmolol? Med Hypotheses. 2016;87:44–47.
41. Barone FC, Campbell WG Jr, Nelson AH, Feuerstein GZ. Carvedilol prevents severe hypertensive cardiomyopathy and remodeling. J Hypertens. 1998;16:871–84.
42. Landmesser U, Cai H, Dikalov S, McCann L, Hwang J, Jo H, et al. Role of p47(phox) in vascular oxidative stress and hypertension caused by angiotensin II. Hypertension. 2002;40:511–5.
43. Taniyama Y, Griendling KK. Reactive oxygen species in the vasculature: molecular and cellular mechanisms. Hypertension. 2003;42:1075–81.
44. Pechánová O. Contribution of captopril thiol group to the prevention of spontaneous hypertension. Physiol Res. 2007;56 (Suppl. 2):S41–S48.
45. Niazi ZR, Silva GC, Ribeiro TP, León-González AJ, Kassem M, Mirajkar A, et al. EPA:DHA 6:1 prevents angiotensin II-induced hypertension and endothelial dysfunction in rats: role of NADPH oxidase- and COX-derived oxidative stress. Hypertens Res. 2017;40:966–75.
46. Yoshida J, Yamamoto K, Mano T, Sakata Y, Nishikawa N, Nishio M, et al. AT1 receptor blocker added to ACE inhibitor provides benefits at advanced stage of hypertensive diastolic heart failure. Hypertension. 2004;43:686–91.
47. Agabiti-Rosei C, Favero G, De Ciuceis C, Rossini C, Porteri E, Rodella LF, et al. Effect of long-term treatment with melatonin on vascular markers of oxidative stress/inflammation and on the anticontractile activity of perivascular fat in aging mice. Hypertens Res. 2017;40:41–50.
48. Bukowska A, Hammwöhner M, Sixdorf A, Schild L, Wiswedel I, Röhl FW, et al. Dronedarone prevents microcirculatory abnormalities in the left ventricle during atrial tachypacing in pigs. Br J Pharmacol. 2012;166:964–80.
49. Veskoukis AS, Nikolaidis MG, Kyparos A, Kouretas D. Blood reflects tissue oxidative stress depending on biomarker and tissue studied. Free Radic Biol Med. 2009;47:1371–4.
50. González J, Valls N, Brito R, Rodrigo R. Essential hypertension and oxidative stress: new insights. World J Cardiol. 2014;6:353–66.
51. Ruiz-Hurtado G, Condezo-Hoyos L, Pulido-Olmo H, Aranguez I, Gónzalez MC, Arribas S, et al. Development of albuminuria and enhancement of oxidative stress during chronic renin-angiotensin system suppression. J Hypertens. 2014;32:2082–91.
52. Rodríguez-Rodríguez P, López de Pablo AL, Condezo-Hoyos L, Martín-Cabrejas MA, Aguilera Y, Ruiz-Hurtado G, et al. Fetal undernutrition is associated with perinatal sex-dependent alterations in oxidative status. J Nutr Biochem. 2015;26:1650–9.
53. Fan NC, Tsai CM, Hsu CN, Huang LT, Tain YL. N-acetylcysteine prevents hypertension via regulation of the ADMA-DDAH pathway in young spontaneously hypertensive rats. Biomed Res Int. 2013;2013:696317.
54. Quintana-Villamandos B, González MC, Delgado-Martos MJ, Condezo-Hoyos L, Boger RH, Luneburg N, et al. Short-term esmolol attenuated remodeling of the thoracic aorta in hypertensive rats by decreasing concentrations of ADMA down-regulated by oxidative stress. Eur J Pharmacol. 2016;791:502–9.